# Characterization of hydroxyl groups on water-reacted Si ( 001 ) – 2 x 1 using synchrotron radiation O 1 s core-level spectroscopies and core-excited state density-functional calculations

S. Carniato, J.-J. Gallet, F. Rochet, G. Dufour, F. Bournel, S. Rangan, A. Verdini, L. Floreano

# Characterization of hydroxyl groups on water-reacted Si(001)-2×1 using synchrotron radiation O 1*s* core-level spectroscopies and core-excited state density-functional calculations

S. Carniato, J.-J. Gallet, F. Rochet,* G. Dufour, and F. Bournel
*Laboratoire de Chimie Physique Matière et Rayonnement, Université Pierre et Marie Curie, 11 rue Pierre et Marie Curie, 75231 Paris Cedex 05, France*

S. Rangan†
*Rutgers University, Department of Physics and Astronomy, 136 Frelinghuysen Road, Piscataway, New Jersey 08854, USA*

A. Verdini and L. Floreano
*Laboratorio Nazionale TASC-INFM, s.s. 14 km 163.5 in Area Science Park, 34012 Trieste, Italy*
(Received 16 March 2007; revised manuscript received 19 June 2007; published 14 August 2007)

The system constituted by the Si(001)-2×1 surface exposed to water molecules at room temperature has been chosen to single out the electron structure of the hydroxyl SiOH, a surface species playing an important role in many technologically relevant processes. We confront here original core-electron spectroscopy density functional theory (DFT) calculations to synchrotron radiation O 1*s* x-ray photoelectron spectroscopy (XPS) and (polarization-dependent) near-edge x-ray absorption spectroscopy (NEXAFS) data. Using clusters to mimic the silicon surface, various SiOH environments (unpaired and paired hydroxyls) have been examined. The impact of the hydrogen bond on the calculated core-ionized and/or neutral core-excited states is examined, and compared to the limit case of the water dimer. The theoretical approach enables us to label the main experimental NEXAFS transitions and to interpret their polarization-dependent dichroism. As water dissociation on the surface can go beyond the formation of hydroxyls, the DFT electron structure of bridging oxygens (SiOSi) is calculated. It is predicted that the XPS line associated to the latter species is shifted by 0.5–1.0 eV to lower binding energy with respect to that of the hydroxyls. Then, on this basis, the reconstruction of the experimental O 1*s* XPS spectrum can provide the relative distribution of hydroxyls and of the bridging oxygens (a minority species). The present work paves the way for future spectroscopic works examining the bonding and reactiveness of hydroxyls with other molecular species.

DOI: 10.1103/PhysRevB.76.085321 PACS number(s): 68.43.Fg, 81.05.Cy, 81.65.Mq, 82.30.Rs

## I. INTRODUCTION

The controlled functionalization of the "technological" Si(001)-2×1 surface by hydroxyls (Si-OH), would open new, interesting, avenues in the realm of silicon-based technologies. For instance, the formation of a surface layer of hydroxyls on top of the silicon appears as the "ideal" starting point in the atomic layer deposition process of high-permittivity metal oxides dielectrics, based on ligand-exchange reaction.[1] In effect, it is desirable to decrease as much as possible the thickness of the interfacial silicon oxide layer for the obvious reason of increasing the effective capacitance. Second, the presence of surface hydroxyls enables the selective grafting of a multifunctional organic molecule (via a water elimination reaction with suitable organic functionalities[2]) without incurring the risk of multiple adsorption geometries, generally observed in the case of adsorption on the clean surface.[3]

Hydroxylation of the clean surface can be envisaged as complete or partial. The chemical steps leading to complete hydroxylation (one monolayer of OH) are not firmly established yet.[4] On the other hand, the partial hydroxylation of the clean Si(001)-2×1 surface (around half a monolayer of OH is formed), that is simply realized by direct exposure to $H_2O$ from a temperature of 110 K, is well documented.[5] It is the typical case study that has enormously benefited from the use of various surface characterization tools, whose data interpretations can be therefore cross-checked. Infrared (IR) vibrational spectroscopy studies by Chabal *et al.*[6] indicate that the majority product is a H-Si-Si-OH unit, resulting from the fragmentation of water on two dangling bonds pertaining to the same dimer.[7] This view has been confirmed by scanning tunneling microscopy (STM) images.[8,9] For its part, Si 2*p* XPS spectroscopy[10] shows that the latter picture is valid, provided that room temperature exposures do not exceed a few (1 L=$10^{-6}$ Torr×s), a dose above which oxidation states higher than $Si^{1+}$ begin to appear. When located on the same side of the dimer row, hydroxyls are close enough to interact via hydrogen bonding. Combining a vibrational spectroscopy analysis of the Si-H and O-H stretching frequencies to DFT cluster calculations Gurevich *et al.*[11] came to the conclusion that "the water-exposed Si(100)-(2×1) surface [at a temperature of 220 K (Ref. 12)] is comprised of a mixture of single dimers with isolated hydroxyl groups and paired dimers that are coupled by hydrogen bonding between OH groups on neighboring dimers in the same row of the reconstructed 2×1 surface." (OH pairing may be the cause of OH bond alignment, detected at ~200 K by the surface-sensitive technique called electron stimulated desorption ion angular distributions.[13,14]) OH pair formation is indeed possible due to the distribution of hydroxyls along the dimer row, as seen in the STM images obtained by Chander *et al.*[9] at 300 K. In an image obtained at saturation coverage, the Si-OH and Si-H moieties can be distinguished by their dif-

 

ferent brightness. No long range order is seen: OH groups are located on the same side of a dimer row for limited spans of a few dimers, these features coexisting with extended regions of OH groups on opposite ends of neighboring dimers in a row.

Theoretical calculations—using silicon clusters to mimic the silicon surface—disagree about the intensity of the hydrogen bond between two adjacent hydroxyls. On the one hand, density functional theory (DFT) points to a weak hydrogen bond. The energy gain due to OH pairing is small, around 2 kcal/mol (Ref. 15) (86.7 meV)—see Refs. 11 and 16—and the O-O distance is reduced from 3.85 Å (the {110} lattice spacing) to 3.67 Å.[16] This energy and distance are at the limits of typical hydrogen bond parameters in liquids or the gas phase (the hydrogen bond strength and O-O distance in water dimer are 3.09 kcal/mol (Ref. 17) (134.0 meV) and 2.976 Å,[18] respectively). On the other hand, Hartree-Fock (HF) calculations, taking account correlation corrections at the second-order Møller-Plesset perturbation level of theory (MP2) (Ref. 19) indicate a stronger H bonding. The calculated hydrogen bond length is 1.96 Å using the HW(*d*) basis set, which would correspond to a maximum O-O distance of 2.92 Å (respectively, 3.28 Å), assuming a linear H bond and a O-H distance 0.96 Å. This would correspond to a sizeable twist of the Si-O bond out of the {110}-type azimuthal plane containing the dimer bond (the O-O distance would be reduced by around 0.30–0.45 Å). It can be noticed, however, that such a large twist is not accounted for by O 1*s* photoelectron diffraction data analysis.[20]

While the characterization of the chemical products of water on Si(001)-2×1 has essentially relied on vibrational spectroscopies,[6,11,21–23] so far the use of O 1*s* core spectroscopies—x-ray photoelectron spectroscopies (XPS) and/or near-edge x-ray absorption fine structure (NEXAFS) spectroscopy—remains scarce. No such occurrence is found in the review by Henderson, dating back to 2002,[5] and only a photoion-photoelectron spectroscopy study at the O 1*s* edge can be mentioned.[24] In fact, XPS (Ref. 25) and NEXAFS (Ref. 26) give useful information on the chemical environment of a given atom. Moreover NEXAFS, which is a spectroscopy of the unoccupied states, also enables the determination the orientation in space of the adsorbate molecular orbitals.[27] XPS and NEXAFS spectroscopies allow the determination of "frozen-in-time" local structures since the spectroscopic process takes place on an orders-of-magnitude faster time scale than the motion of the hydroxyls.

In the present study, the Si(001)/$H_2O$ system has been chosen to single out the electron structure of the silanol-like surface species. We confront here original core-excited state DFT calculations to experimental O 1*s* XPS and polarization-dependent NEXAFS spectroscopy data, obtained with an unprecedented resolution.[28] Our methodology is the same as that used in a series of papers aiming at characterizing the adsorption modes of ($\pi$-bonded) organic molecules on Si(001)-2×1 (Refs. 29 and 30) and Si(111)-7×7.[31]

The paper is organized as follows. In Sec. II we present the experimental XPS/NEXAFS spectra of the water dosed Si(001)-2×1 surface. In Sec. III we give the computation results of O 1*s* ionization potential (IP) and NEXAFS transition energies for various reaction products of water, using silicon clusters to mimic the dimerized silicon surface. First, we have considered the H-Si-Si-OH unit. We have taken into account recent theoretical works showing that the H bond in the water dimer induces major modifications in the O 1*s* NEXAFS (Ref. 32) and XPS (Ref. 33) spectra with respect to those of the isolated molecule. Therefore we have calculated the O 1*s* NEXAFS spectrum of hydroxyls, isolated, and in interaction via H bond. Second, to account for the presence of a minority species detected in the O 1*s* XPS spectra, we have calculated the NEXAFS transitions and IP of the H-Si-O-Si-H unit (the inserted oxygen), a model suggested by the STM images of Ref. 9. Finally in Sec. IV the DFT simulations are compared to experiment. Results are summarized in Sec. V, and some possible directions for future research are proposed.

## II. EXPERIMENTAL PART

### A. Experimental details

#### 1. Sample preparation

(001) oriented Si samples are cut into phosphorus doped wafers of resistivity 0.003 Ω cm. They are cleaned from their native oxide by flashing at 1250 °C after degazing 12 h at 650 °C. It is well known that on-axis "nominal" (001) surfaces consist of 2×1 and 1×2 domains in equal proportions, with the dimer rows of one domain running perpendicular to the dimer rows of the other.

Pure water was purified by several freeze-pump-thaw cycles and dosed onto the silicon surface at room temperature, through a leak-valve under constant pressure in the $10^{-8}$–$10^{-7}$ Torr range (the gauge reading being uncorrected).

#### 2. Synchrotron radiation spectroscopies

The experiments have been performed at the ALOISA beamline, ELETTRA synchrotron facility, Trieste, Italy.[34] The insertion device yields linearly polarized light. The photon beam is directed at grazing incidence (6°) to the sample surface.

To measure the XPS spectra, we used a hemispherical (33 mm mean radius) with an acceptance angle of 1° and an energy resolution of 1.7% of the pass energy (for further details on its performances and geometry, see Ref. 35). The spectrometer was always maintained positioned exactly normal to the surface (i.e., 83° from the photon beam, 6° from the electric field direction, within the scattering plane). Core-level (Si 2*p*, O 1*s*) and valence band photoemission spectra have been recorded. The overall experimental resolution (including photon and spectrometer contributions) is about 200 meV at $h\nu$=145 eV and about 390 meV at $h\nu$=660 eV. To ease the visualization of the suboxide states in the Si 2*p* spectrum, the Si $2p_{1/2}$ component of the Si 2*p* XPS spectra is removed numerically,[36] after subtraction of a Shirley background. To do this, we assume a $2p_{3/2}$:$2p_{1/2}$ branching ratio of 2 (the statistical ratio) and a spin-orbit splitting of 0.6 eV. The experimental binding energies are referenced with respect to the Fermi level (the Si $2p_{3/2}$ binding energy is

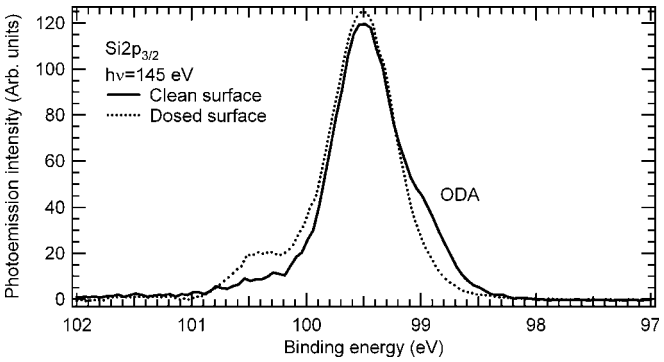


FIG. 1. Experimental Si $2p_{3/2}$ photoemission spectra of the two-domain Si(001) surface before and after exposure to water at room temperature (1.5 L). The photon energy $h\nu$ is 145 eV. ODA is the acronym for "outer dimer atom."

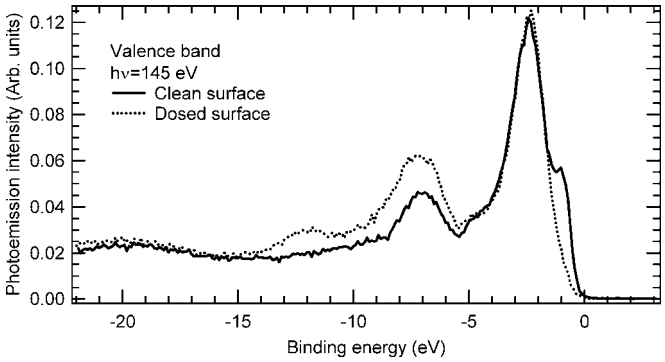


FIG. 2. Experimental valence band spectrum of the two-domain Si(001) surface before and after exposure to water at room temperature (1.5 L). The photon energy $h\nu$ is 145 eV. Note the quenching of the "surface states" (at a binding energy of 0.9 eV) after water dosing.

99.5 eV). Note that the IP is the sum of the binding energy and of the work function.

The O 1*s* NEXAFS spectra were taken in partial yield mode, using a channeltron detector with a retardation potential of 490 V. Polarization dependent NEXAFS measurements are performed at fixed grazing light incidence, by rotating the sample around the manipulator axis, so that the electric field **E** is placed parallel to the silicon surface plane or nearly perpendicular to it (6° away from the sample normal). The photon bandwidth at the O 1*s* edge is 250 meV.

### B. Experiments

#### *1. Adsorption monitoring via Si 2p and valence band spectroscopy*

While the H-Si-Si-OH unit is the dominating species at room temperature for exposures not exceeding around 1 L, surface oxidation, that is oxygen incorporation into the Si-Si dimer bond and backbonds, has been reported for exposures an order of magnitude larger.[10,21,23] As we focus here on the XPS and NEXAFS spectroscopic characterization of the hydroxyl, we have limited the room temperature exposure of the clean Si(001)-2×1 surface to a dose of 1.5 L ($0.75 \times 10^{-8}$ Torr of $H_2O$ for 200 s). Surface oxidation can be controlled by measuring the Si 2*p* core-level in surface sensitive conditions at $h\nu=145$ eV (for photoelectron kinetic energy of 45 eV, that is at their minimum escape depth[37]). The Si $2p_{3/2}$ spectra of the clean and water dosed Si(001)-2×1 surface are compared in Fig. 1. Water adsorption leads to the quenching of the surface core-level state (outer dimer atom) shifted by −0.5 eV (Refs. 38 and 39) from the bulk peak and to the growth of the Si-OH line, shifted by +0.9 eV from the bulk peak. However the Si-OH line cannot be energetically distinguished from a $Si^{1+}$ state resulting from the insertion of an O atom into a Si-Si bond (see, e.g., the experimental work of Jolly *et al.*[40] and the Si 2*p* binding energy calculations of Pasquarello and co-workers[41,42]).

Therefore the occurrence of an O atom bridging two Si atoms, such as in a H-Si-O-Si-H unit, cannot be excluded. On the other hand, oxidation states $Si^{n+}$ with $n \geqslant 2$), whose binding energy shift with respect to the bulk line scales approximately as $n \times 0.9$ eV, are absent from the Si $2p_{3/2}$ photoemission spectrum of Fig. 1. This shows that silicon subsurface oxidation is negligible for the dose we have used (compare with the 20 L Si $2p_{3/2}$ spectrum of Ref. 10). The advancement of the surface reaction can also be followed by the intensity change of the valence band surface states upon water exposure (the spectra are measured at $h\nu=145$ eV and shown in Fig. 2). On the one hand, dissociated water states appear at binding energies in the 5–15 eV range, in agreement with previous valence band spectroscopy data.[43] On the other hand, the surface-state band[44] located around 0.9 eV below the Fermi level, is completely quenched after the exposure of 1.5 L. This shows that most of the dimer dangling bonds are tied up with H/OH fragments.

Combining Si 2*p* core-level and valence band spectroscopy we have shown that for a dose of 1.5 L (i) oxygen attachment is limited to the first silicon plane (with likely a majority of Si-OH species, see Sec. II B 2) that a high coverage situation is reached. Therefore, the two necessary conditions enabling the *possible* manifestation of (same-sided) hydroxyl-hydroxyl interaction in the O 1*s* NEXAFS spectra are fulfilled.

#### *2. O 1s XPS and NEXAFS spectra*

In Fig. 3 we give the O 1*s* XPS spectrum of the water-dosed Si(001)-2×1 surface measured at a photon energy $h\nu=660$ eV. The spectrum has been fitted using Voigt functions [Lorentzian full width at half maximum (FWHM) 0.1 eV, Gaussian FWHM 1 eV] after a Shirley-type background substraction. Two components corresponding to two different chemical environments are clearly seen, a majority one at 532.4 eV and a minority one at 531.4 eV, with a majority:minority spectral weight distribution of 88:12. Therefore the first oxidation state in the Si $2p_{3/2}$ spectrum of Fig. 1 corresponds in fact to two different chemical bondings, a majority species, Si-OH, and minority species that are related to oxidized dimers. The minority peak could be attributed to bridging oxygens (Si-O-Si), on the basis of initial state considerations. Indeed Si is less electronegative than H ($\chi_H=2.2$ and $\chi_{Si}=1.9$ on a Pauling electronegativity scale[45]),

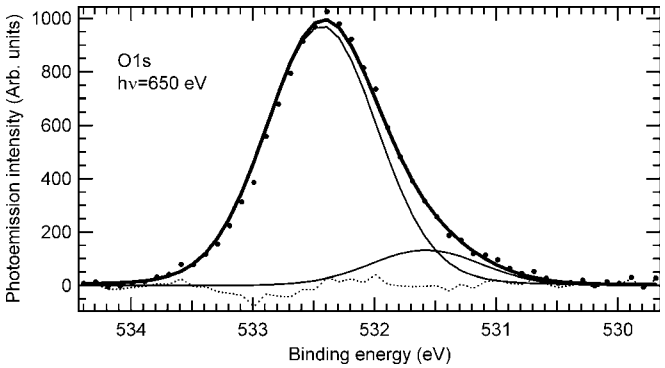


FIG. 3. Experimental O 1*s* XPS spectrum (dots) of the two-domain Si(001) exposed to water (1.5 L) at room temperature. The photon energy $h\nu$ is 660 eV. The best fit (solid line) is also given.

thus there are more electrons around O in Si-O-Si than in Si-OH. Hence the better screening of the O 1*s* core hole in Si-O-Si, and its lower binding energy. A detailed discussion, supported by XPS and NEXAFS DFT calculations, will be given further in the text, in Sec. IV.

The normalized O 1*s* NEXAFS spectra of the Si(001)-2 $\times$1 surface exposed to water at room temperature are given Fig. 4 for two orientation of the electric field **E**, nearly normal and parallel to the surface. The NEXAFS spectra are recorded, while the sample is kept at room temperature. Four main transitions are observed: a weakly dichroic transition at 533.1 eV, a transition strongly polarized normal to the surface at 534.6 eV and two weaker and broader transitions centered at 535.8 and 537.4 eV, whose intensity also increase when **E** is nearly normal to the surface. The FWHM of the transition at 534.6 eV, around 1.5 eV, is much broader than the photon bandwidth of 250 meV.

The silicon surface exposed to water at 300 K was also cooled down to cryogenic temperatures. The lower limit attained was 150 K. At 180 K (that is below the measurement temperature of 220 K at which SiOH pairing is clearly observed by IR spectroscopy) a control XPS measurement—with the present overall energy resolution of 390 meV—did not indicate any noticeable change in the O 1*s* spectral shape with respect to that measured at 300 K. The O 1*s* NEXAFS spectra measured at 150 K (see inset of Fig. 4) presents the same spectroscopic features and dichroic behavior as the one measured at 300 K.

## III. COMPUTATIONAL PART

### A. Computational details

#### *1. Geometry optimization*

Electronic structure calculations were completed with the GAMESS (Ref. 46) software package using Becke three-parameter exchange functional,[47] along with the Lee-Yang-Parr[48] gradient-corrected correlation functional (the so-called B3LYP functional). As far as hydrogen bonding between same-sided, adjacent hydroxyls can be involved in the determination of the bonding geometries, the use the B3LYP functional deserves a comment. In effect, the accuracy of DFT to describe the hydrogen interaction relies on the functional used to approximate the electronic exchange and correlation. Generalized density gradient approximations (GGA) and hybrid functionals are more accurate to describe the hydrogen bonding than local density approximation, which strongly overestimates the hydrogen bond strength.[49] Among the various available GGA functionals to treat the hydrogen bonds, the Becke-Lee-Yang-Parr (BLYP) and the B3LYP have been commonly used. In particular, the BLYP (Ref. 16) and B3LYP (Ref. 11) functionals were used to calculate the effects of hydroxyl coupling on water-dosed Si(001). The B3LYP functional was also used to describe interadsorbate (H-bonding) interactions on ammonia-dosed Si(001).[50] More recently, Guo and co-workers used B3LYP to give a microscopic description of water-alcohol mixtures,

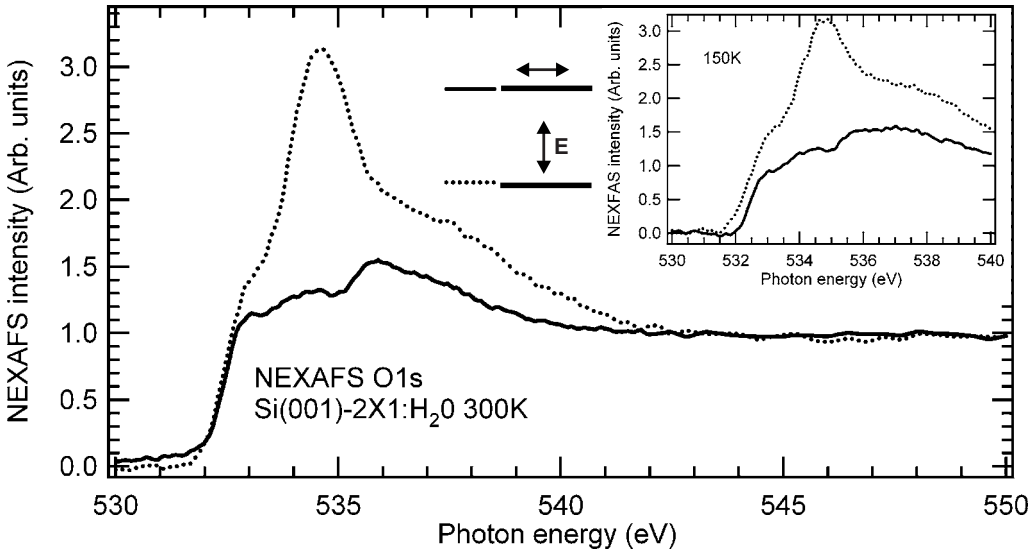


FIG. 4. Normalized experimental NEXAFS spectra of the two-domain Si(001) surface exposed to water (1.5 L) at room temperature (measurement at room temperature). The electric field **E** is oriented either nearly normal (dotted line) or parallel (solid line) to the two-domain silicon surface. Inset: the measurements are performed while the sample temperature is kept at 150 K.

TABLE I. Calculated distances (in Å) and angles (in deg.) for the optimized water dimer (B3LYP). O(*D*) is the oxygen atom that donates its hydrogen, O(*A*) is the oxygen atom that accepts the hydrogen atom

| | O-O distance | H bond length | ∠O(*D*)HO(*A*) |
|---|---|---|---|
| without diffuse function | 2.935 | 1.996 | 162.8 |
| with diffuse function | 2.910 | 1.945 | 172.5 |

prior to x-ray emission calculations.[51] In general, B3LYP calculations are satisfactory for optimizing the geometry of H-bonded molecular clusters, unless the dispersion energy component, not taken into account by this functional, becomes important.[52]

The DFT (B3LYP) geometry optimizations have been performed using 6-311$G^*$ basis sets for O and Si, and a 6-31$G^*$ basis set for H. Larger basis sets have been also used, adding two diffuse functions (*s* and *p* with an exponent equal to 0.0845) to the 6-311$G^*$ basis sets of O and three diffuse functions (one *s* with an exponent equal to 0.036 and two *p* with exponents equal to 0.275 and 0.075, respectively) to the 6-31$G^*$ basis set of H. The use of diffuse functions influences the calculated length of the hydrogen bond. For the water dimer $(H_2O)_2$ the geometrical outputs of the DFT calculation are given in Table I. The H bond is larger for the "small" basis set than for the "large" one supplemented with diffuse functions. The O-O distance of 2.910 Å is in close agreement with the best *ab initio* CCSD(T) study leading to an O-O distance of 2.912±0.005 Å.[53] Note that the calculated O-O distances are all smaller than the experimental value of 2.976 Å,[18] but due to the floppiness of the dimer the latter experimental is in fact a vibrationally averaged value.

To simulate the silicon substrate, silicon clusters of various sizes were used. We first built a one-dimer cluster $Si_9H_{12}$, in which the top two silicon atoms compose the surface dimer, while the remaining seven Si atoms, compose three subsurface layers which are hydrogen terminated to preserve the $sp^3$ hybridization of the bulk diamond lattice. To take into account adsorbate-adsorbate interactions we used a larger cluster encompassing three dimers in a row ($Si_{21}H_{20}$). The top six silicon atoms compose the surface dimer, while the remaining fifteen Si atoms compose three subsurface layers (which are also hydrogen terminated).

#### 2. Core-excited states

The local minima geometries we find for the molecule *plus* Si cluster system are the starting point of the calculation of NEXAFS transitions and ionization potentials (IP). (Note that in the calculation the IP is the binding energy measured from the vacuum level, while experimentally the binding energies are referenced with respect to the Fermi level.) The quantum chemical *ab initio* calculations of the O 1*s* excited states are also performed at a DFT level of theory. We used a modified version of the GAMESS(US) program, enabling (i) the choice of a fractional occupancy for the core-hole and (ii) the calculation of singlet core excited energy values.[54]

The excited atom was described with a large basis set. For O we use the IGLOO-III basis to which we add diffuse functions, three *s* (with exponents 0.0678, 0.0256, and 0.00973), three *p* (with exponents 0.0515, 0.0201, and 0.0078), and three *d* (with exponents 0.0875, 0.0218, and 0.0056). Effective core potentials (SBJK) for the silicons (we have already tested that the use of SBJK functions has a minor effect on the adsorbate IP, see Ref. 29). For all H atoms (those passivating the silicon cluster and those of the adsorbate), a 6-31$G^*$ basis was used, without diffuse functions.

Absolute values of NEXAFS transitions are calculated via the so-called ΔKohn-Sham method (denoted hereafter ΔKS). The energy of the core excited state is calculated by removing one electron from the 1*s* and adding one to the unoccupied molecular orbital (UMO) of interest, i.e., by calculating the NEXAFS state $(1s)^1(\mathrm{UMO})^1$. Then the transition energy is obtained as the difference between the energy of the excited state and that of the ground state. The relativistic correction of 0.4 eV is included, according to Triguero *et al.*[55] The ΔKS triplet final state transition energies are corrected using the sum method of Ziegler, Rauk and Baerends,[56] to account for the spin conservation in dipolar transitions leading to a singlet final state. ΔKS energies have been calculated for the molecular orbitals leading to the major oscillator strengths (computed in the framework of the dipolar approximation). For the calculation of O 1*s* IP, the same ΔKS method is applied, IP being the difference between the energy of the excited state, represented by a core hole in the 1*s* orbital, and that of the ground state.[57]

While this separate state Kohn-Sham scheme is a convenient and accurate option for ionization potential (IP) and first core excited transition energies calculations, it is not always applicable to calculate the whole spectrum, due to problems of collapse in optimizing higher excited states. To circumvent this difficulty, we diagonalize a potential built from orbitals where a 1*s* electron is removed (the full core hole is denoted FCH) and put into one UMO or "distributed" into more UMOs—in the latter case their occupancy is fractional. The excited electronic levels are then determined by the electrostatic field of the remaining molecular system. The eigenvalues and eigenvectors give the full spectrum of excitation energies and moments. The transition energy is simply the difference between the energy of the virtual orbital and that of the 1*s* orbital and the oscillator strengths are obtained from the eigenvectors within the dipolar approximation (see, for instance, Refs. 29–31 and 54).

An *ad hoc* FCH-UMOs potential is found (i) when the relative difference between the various energies corresponds to the calculated ΔKS ones and (ii) when the oscillator strengths (dipolar approximation) compare to those of the ΔKS method. As the absolute values of the energies may be 0.5–1 eV off the ΔKS (and experimental) ones, the NEXAFS spectra are repositioned on an absolute energy scale provided by the energy of the first bound excited state calculated with the ΔKS method. Below the calculated IP, the NEXAFS spectrum consists of the discrete lines calculated by method, broadened by convolution with a Gaussian of 0.8 eV FWHM. For transitions calculated above IP, we convert the discrete lines into a continuum using the Stieltjes

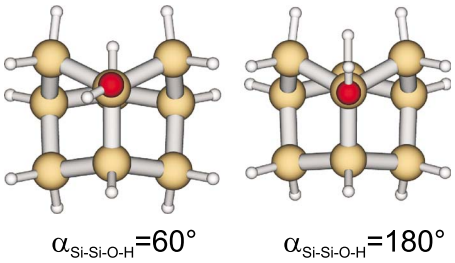


FIG. 5. (Color online) The unpaired hydroxyl [single-dimer cluster ($Si_9H_{12}$) plus (H,OH)]. Two minimum energy conformers are calculated, gauche ($\alpha_{Si\text{-}Si\text{-}O\text{-}H}=60°$) and trans ($\alpha_{Si\text{-}Si\text{-}O\text{-}H}=180°$).

imaging procedure[58] (the calculated continuum cross-section is convoluted with the same Gaussian function used for the discrete part below IP).

### B. Computation results

#### *1. The limit case of strong hydrogen bonding: The water dimer vs the free molecule*

The calculated ΔKS O 1*s* IP of the free molecule (539.78 eV) coincides with the experimentally measured value [539.79 eV (Ref. 59)]. In the water dimer, the formation of a *short* hydrogen bond (see Table I) has a sizeable effect on the calculated IP. The water monomer O 1*s* IP is split into two values, that of the donor (*D*) at lower binding energy (538.61 eV) and that of the acceptor (*A*) at higher binding energy (540.34 eV). Our DFT calculation is in good qualitative accord (in particular with respect to energy ordering) with the CASSF calculation of Felicíssimo *et al.*,[33] but the energy splitting in the CASSF calculation (1.29 eV) is smaller than that found in our DFT calculation (1.9 eV). To our knowledge no experimental O 1*s* IP measurement is available in the literature for the water dimer.

#### *2. Weak hydrogen bonding: Unpaired vs paired hydroxyls*

As discussed in the Introduction, the experimental literature indicates that the H-Si-Si-OH unit (H and OH bound to the same dimer) is the majority product. Indeed, DFT cluster calculations,[16,60] periodic DFT calculations,[61] and post-HF (Ref. 19) cluster calculations confirm that there is no *net* reaction barrier to the formation of this product. The hydroxyls can be paired by hydrogen bonding, or remain unpaired (for instance, when they are placed on opposite ends of adjacent dimers in a row). In a first step, the unpaired hydroxyl is simulated using a one-dimer cluster $Si_9H_{12}$ *plus* water fragments (H,OH). The minimum energy is found for a dihedral angle $\alpha_{Si\text{-}Si\text{-}O\text{-}H}$ of about 60° (the OH is oriented gauche). A (nearly degenerate) secondary minimum is found for the OH oriented trans ($\alpha_{Si\text{-}Si\text{-}O\text{-}H}=180°$), +0.25 kcal/mol (10.8 meV) above the lowest energy geometry. The two conformers are depicted in Fig. 5. The present B3LYP calculations are in good accord with the BLYP calculation ($Si_9H_{12}$ cluster) of Konečný and Doren,[16] who found an absolute minimum energy geometry at $\alpha_{Si\text{-}Si\text{-}O\text{-}H}=62.2°$, and a secondary minimum at $\alpha_{Si\text{-}Si\text{-}O\text{-}H}=180°$ [+0.5 kcal/mol (21.7 meV) above the lowest energy geometry]. Note that the RHF/MP2 approach, used by Jung *et al.*,[19] leads to similar results: two product structures are found, with the OH oriented gauche ($\alpha_{Si\text{-}Si\text{-}O\text{-}H}\sim 60°$) as well as trans ($\alpha_{Si\text{-}Si\text{-}O\text{-}H}\sim 180°$), 0.3–0.4 kcal/mol (13.0–17.3 meV) higher in energy than the gauche form). The calculated rotational barrier calculated in Ref. 19 for the trans-to-gauche isomerization reaction is very small, 0.5–0.6 kcal/mol (21.7–26.0 meV), which means that the OH rotation around the Si-O axis is not kinetically hindered at room temperature.[62]

TABLE II. ΔKS IPs and ΔKS NEXAFS energies (main transitions) for various types of hydroxyls. The "unpaired" hydroxyl is calculated using a $Si_9H_{12}$/(OH,H) cluster. The donor (*D*), acceptor (*A*), and "free" (*F*) species are calculated using a $Si_{21}H_{20}$/3(OH,H) cluster, see Fig. 7. Energies are in eV. In each case, the *L*1 orbital is the LUMO.

| hydroxyl type | cluster type | transition | ΔKS |
|---|---|---|---|
| unpaired | $Si_9H_{12}$/(OH,H) | *L*1 | 532.92 |
| | | *L*2 | 534.50 |
| | | IP | 537.79 |
| *D* | $Si_{21}H_{20}$/3(OH,H) | *L*1 | 533.03 |
| | | *L*2 | 534.09 |
| | | *L*3 | 534.32 |
| | | IP | 537.20 |
| A | | *L*1 | 533.12 |
| | | *L*2 | 534.21 |
| | | *L*3 | 534.40 |
| | | IP | 537.45 |
| F | | *L*1 | 533.35 |
| | | IP | 537.73 |

For the "$Si_9H_{12}$ plus (H,OH)" cluster (unpaired hydroxyl), the first two main ΔKS O 1*s* transitions (labeled *Li* with $i=1,2$) are reported in Table II [note that *L*1 corresponds to the lower unoccupied molecular orbital (LUMO)]. Their values, that are marginally affected by changes in $\alpha_{Si\text{-}Si\text{-}O\text{-}H}$, are found close to the two main experimental transitions shown in Fig. 4.

The absorption spectra, simulated with the $(1s)^1(L1)^{1/2}(L2)^{1/2}$ FCH-UMOs potential, are presented in Fig. 6. Note that the calculated curves take into account the fourfold symmetry of a two-domain silicon surface, and therefore can be compared directly to the experimental spectra of Fig. 4. To take into account the presence of two rotamers, curve (c) of Fig. 6 is the weighted sum of the two upper curves, using a gauche:trans ratio of 60:40 calculated (via a Boltzmann factor) at 300 K for a potential energy difference between conformers of 0.25 kcal/mol (10.8 meV). The averaged curve is indeed equivalent to the one obtained with a dihedral angle $\alpha_{Si\text{-}Si\text{-}O\text{-}H}$ intermediate between 60° and 180°, that is about 90°. This means the averaged OH bond direction of the unpaired hydroxyl is nearly orthogonal to the Si-Si dimer axis. With respect to curve (c), the simulated curve corresponding to the low tem-

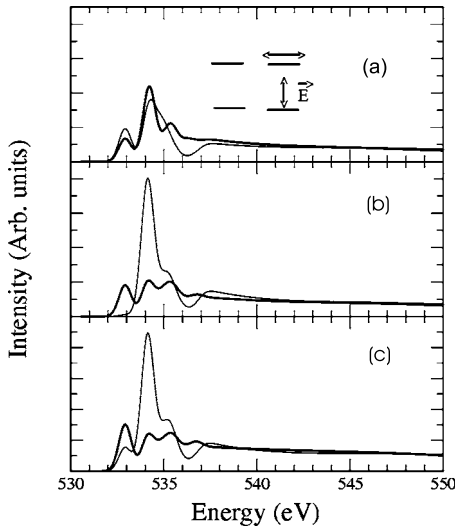


FIG. 6. Simulation of the O 1s NEXAFS spectra for the unpaired hydroxyl [$(Si_9H_{12})$ cluster] using the $(1s)^1(L1)^{1/2}(L2)^{1/2}$ FCH-UMOs potential (the spectra are rescaled energetically using the ΔKS NEXAFS energies given in Table II). Curve (a) corresponds to the $\alpha_{\text{Si-Si-O-H}}=60°$ conformer, curve (b) to the $\alpha_{\text{Si-Si-O-H}}=180°$ conformer. Curve (c) is the weighted sum of the (a) and (b) curves assuming a gauche:trans distribution of 60:40 (see text). The fourfold symmetry of the two-domain silicon surface is taken into account. The thick (thin) line corresponds to **E** parallel (perpendicular) to the silicon surface.

perature case should not be that different as the gauche:trans ratio is 70:30 at 150 K. A detailed discussion, confronting simulation to experiment and embracing all the envisaged adsorption models, will be given further in the text, in Sec. IV.

The effect of hydrogen bonding between hydroxyls has been examined using a large cluster comprising three dimers in a row, the hydroxyls being placed on the same side of the dimer row. The "$Si_{21}H_{20}$ plus 3(H,OH)" cluster is depicted in Fig. 7. The geometrical outputs of the DFT/B3LYP optimization, most relevant to the discussion, are reported in Table III. Independently of the use or not of diffuse functions, two hydroxyls, *D* (for donor) and *A* (for acceptor) pair up, due to H bonding, and therefore have fixed dihedral angles $\alpha_{\text{Si-Si-O-H}}$ of around 85°. The third one *F* is left free (compare with the

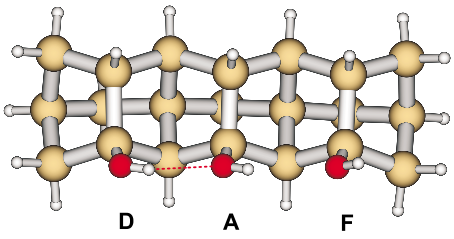


FIG. 7. (Color online) Three-dimer cluster $(Si_{21}H_{20})$ plus 3(H,OH). The oxygens are labeled *D* ("donor"), *A* ("acceptor"), and *F* ("free"). A H bond is established between O(*D*) and O(*A*). On the other hand, no H bond forms between O(*A*) and O(*F*). The H bond length [H(*D*)-O(*A*) distance] and O(*D*)-O(*A*) distance depend on the fact that the basis sets are supplemented by diffuse functions or not (see Table III).

TABLE III. DFT/B3LYP calculated distances (Å) and angles (degrees) for the optimized geometries of the three-dimer cluster $(Si_{21}H_{20})$ plus 3(H,OH). O and H labeling is given in Fig. 7. "fcn" is for function. For comparison we give the values from MP2/HW(*d*) obtained by Jung *et al.* (Ref. 19) with a $Si_{48}H_{36}$/3(H,OH) cluster.

| | B3LYP without diffuse fcn | B3LYP with diffuse fcn | MP2 Jung *et al.* |
|---|---|---|---|
| $d_{\text{H}(D)\text{O}(A)}$ | 2.725 | 2.504 | 2.08 |
| $d_{\text{O}(D)\text{O}(A)}$ | 3.563 | 3.373 | |
| $d_{\text{H}(A)\text{O}(F)}$ | 2.973 | 2.980 | 3.04 |
| $d_{\text{O}(A)\text{O}(F)}$ | 3.746 | 3.765 | |
| $\alpha_{\text{Si-Si-O}(D)\text{-H}(D)}$ | 85.2 | 86.8 | 84.1 |
| $\alpha_{\text{Si-Si-O}(A)\text{-H}(A)}$ | 82.7 | 83.4 | 80.4 |
| $\alpha_{\text{Si-Si-O}(F)\text{-H}(F)}$ | 66.3 | 65.4 | 66.8 |

$Si_9H_{12}$ calculation), with $\alpha_{\text{Si-Si-O-H}}$ of around 66.3°). The three-dimer cluster gives the opportunity of calculating IP and NEXAFS transitions of donor, acceptor and quasi-isolated OH, with the same silicon cluster, therefore avoiding the risk of energy shifts due to variations in cluster size.[57] The use of diffuse function augmented basis sets leads to a shorter hydrogen bond length $d_{\text{H}(D)\text{O}(A)}$ than that calculated with standard basis sets. This trend was already noticed for the water dimer.

The previous DFT cluster calculation by Konečný and Doren[16] and the present one point to weak hydrogen bonding between adjacent hydroxyls. The shortest $d_{\text{H}(D)\text{O}(A)}$ value we find (using diffuse functions) is 2.504 Å, a value much larger than the H bond in the water dimer (1.945 Å). Periodic DFT calculations lead also to an oxygen-oxygen distance between paired hydroxyls [$d_{\text{O}(D)\text{O}(A)}=3.527$ Å (Ref. 63)] close to the one we have calculated with a silicon cluster. On the other hand, in contrast with the DFT calculations, the HF MP2/HW(*d*) calculation of Jung *et al.*[19] (distances and angles are reported in Table III)—using a three dimer cluster $Si_{48}H_{36}$—lead to much less stiff Si-O bonds as the $d_{\text{H}(D)\text{O}(A)}$ value is 2.08 Å, a value only 0.13 Å larger than that of the H bond in $(H_2O)_2$.[64]

To calculate O 1*s* core-excited states we have used the atomic positions provided by the DFT/B3LYP approach, using the basis set supplemented by diffuse functions. Naturally the trends associated to the formation of a (weak) H bond we observe here should be amplified by shorter $d_{\text{H}(D)\text{O}(A)}$ values.

We give in Figs. 8 and 9 the contour plots of antibonding molecular orbitals calculated for core-excited oxygens [$(1s)^1(\text{UMO})^1$ state] pertaining to the *D* and *A* hydroxyls, respectively. For each type of hydroxyl, the depicted antibonding orbitals, labeled *L*1, *L*2, and *L*3, correspond to the three major $1s\rightarrow$UMO transitions. Their ΔKS energies and oscillator strengths are collected in Table II.

Despite their different atomic environments, the *Li* ($i=1,2,3$) molecular orbitals of *D* and *A* hydroxyls present similar features. Due to the difference in electronegativity of the oxygen atom ($\chi_O=3.4$ on a Pauling electronegativity

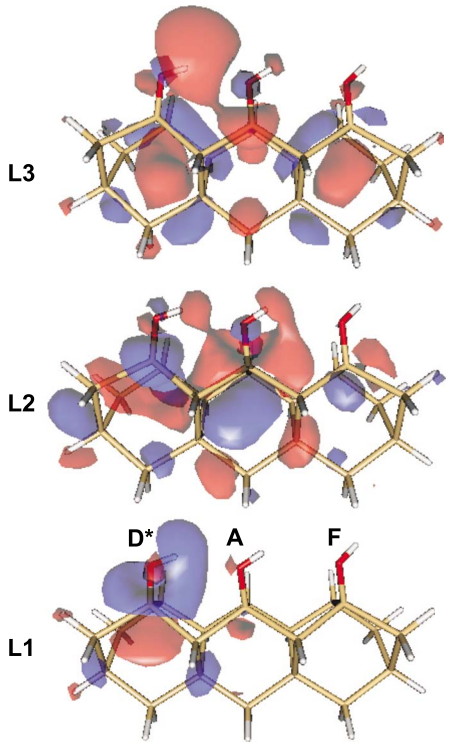


FIG. 8. (Color online) Core-excited donor OH ($D^*$). Contour plots of KS molecular orbitals ($L1$,$L2$,$L3$) to which the electron is promoted.

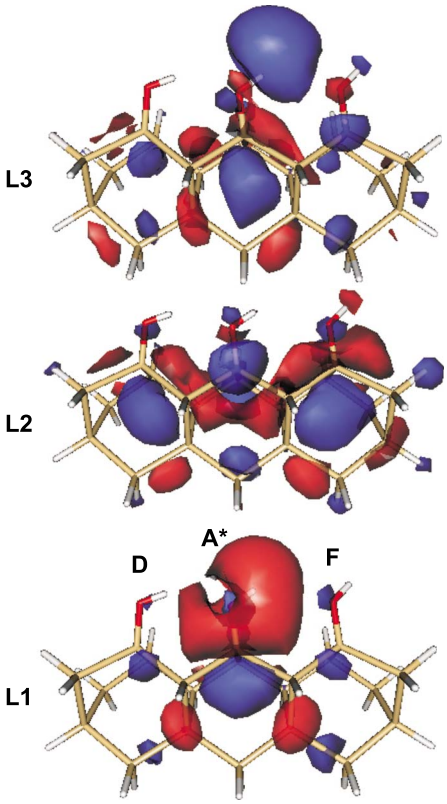


FIG. 9. (Color online) Core-excited acceptor OH ($A^*$). Contour plots of KS molecular orbitals ($L1$,$L2$,$L3$) to which the electron is promoted.

scale[45]), on the one hand, and hydrogen ($\chi_H$=2.2) and silicon ($\chi_{Si}$=1.9) atoms, on the other hand, the antibonding orbitals $L1$ and $L3$ (respectively, $L2$) are strongly polarized towards the hydrogen (respectively, the silicon) atom to which the core-excited oxygen is bonded. Indeed, the $4a_1^*$ orbital of molecular water bears resemblance to the $L1$ (LUMO) orbital of the (core-excited) hydroxyls, while the $2b_1^*$ orbital of water is "split" into the $L2$ and $L3$ hydroxyl orbitals, due to the nonequivalence of O-Si and O-H bonds. Transitions $1s \rightarrow L2$ and $1s \rightarrow L3$ are, nevertheless, nearly degenerate in energy (see Table II). It is clear from Figs. 8 and 9 that the orientation in space of the $p$ components will give a dichroic absorption signal (e.g., the $p$ component of $L3$ tend to be aligned with the Si-OH bond direction, forming a "$\sigma_{Si\text{-}OH^*}$" bond). As expected, H bonding modifies the shape of the molecular orbitals [e.g., the $L3$ orbital of the OH($D^*$) expands over the adjacent OH($A$)].

For $A$, $D$, and $F$ species, the calculated ΔKS NEXAFS energies associated with the main transitions (Table II) cluster around two values 533.20±0.15 eV ($L1$) and 534.25±0.15 eV ($L2$ and $L3$). In particular, we note that the calculated NEXAFS transitions of the $A$ species are shifted by only +0.1 eV with respect to those of $D$ species. The large $d_{H(D)O(A)}$ value explains this small energy change. Indeed, for the molecular water dimer,[32] the donor electronic structure is strongly affected by H bonding as $4a_1^*$ and $2b_1^*$ orbitals mix. The unpaired hydroxyl calculated with the small cluster ($Si_9H_{12}$) gives two main ΔKS NEXAFS transition energies (532.92 and 534.5 eV) close in energy to the corresponding ones for the $A$, $D$, and $F$ species. All in all, the two main experimental transitions at $h\nu$=533.1 eV and $h\nu$=534.6 eV (Fig. 4) are well accounted for by our ΔKS calculations, whatever the cluster type used.

OH pairing has stronger effects on the calculated IP energies. $D$, $A$, and $F$ species present increasing IPs in this order. The IP of the $D$ species is found at lower binding energy than that of the $A$ species (the energy distance is 0.3 eV), reproducing the trend observe for $(H_2O)_2$ (see Sec. III B 1). The IP of the $F$ species (537.73 eV) is separated from that of the $D$ species by about 0.6 eV. "Edge effects"—more specifically a decreased core-hole screening efficiency for a species placed at the extremity of the $Si_{21}H_{20}$ cluster—could account for an increase in the IP, but this effect should not be larger than +0.1 eV.[65]

For the $D$ and $A$ species we have used the $(1s)^1(L1)^{1/2}(L2)^{1/2}$ FCH-UMOs potential. The calculated NEXAFS spectra are given in Fig. 10. Here again the calculated curves take into account the fourfold symmetry of a two-domain silicon surface so as to enable a direct comparison with the experimental spectra of Fig. 4. We draw the attention of the reader to the fact that the dichroic behavior of the $AD$ pair curve [Fig. 10(c)] is similar to that of the averaged "gauche/trans" curve [Fig. 6(c)] of the unpaired hydroxyl.

### *3. H-Si-O-Si-H*

In addition to the H-Si-Si-OH unit, other (minority) products resulting from the complete dissociation of water are

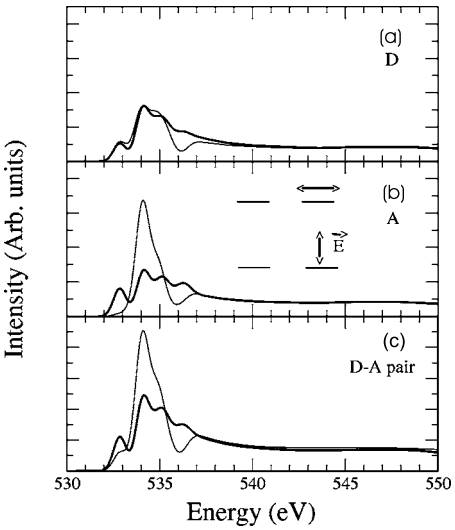


FIG. 10. Simulation of the O 1*s* NEXAFS spectra for the donor (*D*) species [curve (a)] and acceptor (*A*) species [curve (b)] using the optimized geometry of the "$Si_{21}H_{20}$ plus 3(H,OH)" cluster. Curve (c) corresponds to the *AD* pair, that is the average of curve (a) and (b). The $(1s)^1(L1)^{1/2}(L2)^{1/2}$ FCH-UMOs potential is used. The fourfold symmetry of a two-domain silicon surface is taken into account. The thick (thin) line corresponds to **E** parallel (perpendicular) to the silicon surface.

found on the surface at saturation. Limiting ourselves to $Si^{1+}$ oxidation state species (higher oxidation states are not observed for a dose limited to 1.5 L), H-Si-O-Si-H units (one oxygen inserted into the dimer bond) or H-Si-Si(O)H units (one oxygen inserted into a dimer backbond) must be considered. Among other surface oxidized species, H-Si-O-Si-H is detected by IR spectroscopy after prolonged exposures to water (200 L at 373 K).[23] It is also the decomposition product of the H-Si-Si-OH unit at 675 K,[66] as the Si-Si dimer bond (not the backbond) is the target of O insertion. In the absence of calculated images, STM does not provide firm conclusions about the nature of oxidized Si-Si bonds. Bright protrusions (about 10% of the dimers) attributed to "oxidation features" appear at saturation coverage.[9] Their shapes are either asymmetric—localized on a single dimer atom—or symmetric—straddling the whole dimer. One may attribute the latter defects to H-Si-O-Si-H species, but a recent STM work tends to prove that the inserted oxygen should appear dark.[67]

The insertion of oxygen atoms into the silicon-silicon bonds has also been examined at the theoretical level. DFT/B3LYP calculations by Stefanov and Raghavachari[68] indicate that H-Si-O-Si-H is 8 kcal/mol (346.9 meV) more stable than H-Si-Si(O)H, while more recent ones by Watanabe and co-workers[69] point to nearly equal energies (the H-Si-O-Si-H is only 0.04 kcal/mol (1.7 meV) more stable than H-Si-Si(O)H]. Calculated energy barriers (see Ref. 69), determined from the (metastable) H-Si-Si-OH species energy, are high for both types of inserted oxygen, 62.57 kcal/mol (2713.0 meV) for the H-Si-O-Si-H species and 54.39 kcal/mol (2358.5 meV) for the H-Si-Si(O)H one. Generally speaking, simulations do not account for the experimentally observed formation of inserted oxygens at room

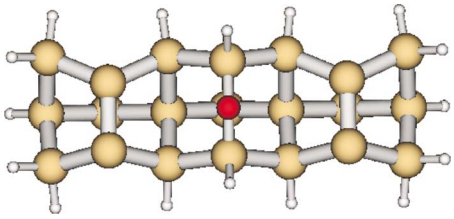

FIG. 11. (Color online) Three dimer cluster $Si_{21}H_{20}$ plus O,2H. The oxygen atom is inserted in the central silicon dimer. Note that the nonreacted dimers remain buckled.

temperature (and even at cryogenic temperature, see Ref. 10). In particular, we note that no theoretical approach considers the possible capture, by an OH species, of a substrate electron (e.g., tunneling from silicon or falling from the conduction band) to form a more stable $OH^-$, which would lower the reaction barrier.

We have chosen to calculate the geometry and the core-excited energetics of the H-Si-O-Si-H unit, taken as representative of an O-inserted species. We used two types of cluster, the small single dimer cluster "$Si_9H_{12}$ plus (O,2H)" and the larger three-dimer "$Si_{21}H_{20}$ plus (O,2H)" cluster, so as to avoid cluster size effects when comparison is made with the hydroxyl simulations. For the small single-dimer cluster the oxygen is symmetrically bonded to the two Si atoms forming the dimer. In the case of the large three-dimer cluster the O atom is inserted within the central Si-Si dimer (Fig. 11). The energy minimization procedure yielded a geometry in which the non-reacted Si dimers remained asymmetric. This induces a slight asymmetry of the Si-O-Si unit. However, changing the cluster size induces small variations in bond lengths (less than 0.02 Å) and angles (less than 3°), as shown in Table IV.

We report in Table V the IP and the main ΔKS O 1*s* transitions, labeled $Li'$ with $i=1,2$, according to the names of the involved UMOs (note that $L1'$ is the LUMO). Cluster effects are small (compare the $L1'$ and IP values), not exceeding 0.25 eV. Note that the calculated NEXAFS transitions of the bridging O (H-Si-O-Si-H) $L1'$ ($L2'$) are close in energy to their counterparts $L1$ ($L2/L3$) of the Si-OH unit. However, the theoretical IP of the bridging oxygen is found systematically smaller than that of the various hydroxyls.

We illustrate the spatial extension of the antibonding molecular orbitals calculated for the core-excited oxygen [$(1s)^1(\mathrm{UMO})^1$ state], showing their contour plots in Fig. 12

TABLE IV. Calculated distances and angles for the H-Si-O-Si-H optimized geometries.

| | H-Si-O-Si-H model |
|---|---|
| $d_{SiO}$ | 1.68[a] (1.66[b]) |
| $d_{SiH}$ | 1.49[a] (1.49[b]) |
| ∠SiOSi | 139.6[a] (137.0[b]) |
| ∠OSiH | 106.7[a] (108.4[b]) |

[a]Calculation using a $Si_9H_{12}$ cluster.
[b]Using a $Si_{21}H_{20}$ cluster. Distances are given in Å and angles in deg.

TABLE V. ΔKS IPs and ΔKS NEXAFS energies (eV) for the H-Si-O-Si-H unit, using either a single-dimer cluster ($Si_9H_{12}$) or a three-dimer cluster ($Si_{21}H_{20}$).

| H-Si-O-Si-H cluster type | transition | ΔKS |
|---|---|---|
| $Si_9H_{12}$/(O,2H) | $L1'$ | 532.55 |
| | IP | 536.95 |
| $Si_{21}H_{20}$/(O,2H) | $L1'$ | 532.70 |
| | $L2'$ | 534.15 |
| | IP | 536.70 |

(as a three-dimer $Si_{21}H_{20}$ cluster is used, the Si-O-Si unit is not fully symmetric). These antibonding orbitals bear strong resemblance with the antibonding orbitals of $H_2O$: the $4a_1^*$ orbital corresponds to $L1'$, while $2b_1^*$ corresponds to $L2'$. Given the space orientation of the $p$-shaped orbitals, the $L1'$ and $L2'$ transitions are strongly polarized. $L1'$ is maximum when the electric field (**E**) is perpendicular to the surface. On the other hand $L2'$ is most intense when **E** is parallel to the surface and orthogonal to the dimer row direction.

We give in Fig. 13 the NEXAFS spectra simulated with a $(1s)^1(L1')^{1/2}(L2')^{1/2}$ FCH-UMOs potential. As in Figs. 6 and 10 the calculated curves take into account the fourfold symmetry of a two-domain silicon surface so as to enable a direct comparison with the experimental spectra. The transition at 532.7 eV (534.2 eV) are polarized perpendicular (parallel) to the surface. The dichroic behavior is the opposite of the (fourfold symmetry averaged) behavior of the hydroxyl counterparts, that show up at about the same energies.

## IV. COMPARISON BETWEEN EXPERIMENT AND SIMULATION

We recall that the experimental O 1$s$ XPS spectrum of the silicon surface exposed to water (Fig. 3) can be reconstructed by two broad peaks (around 1 eV FWHM), a main line at a binding energies of 532.4 eV (88% of the spectral weight) and a minority line at 531.4 eV (12% of the spectral weight). The main peak can be readily put in relation with Si-OH species. Its broadness can be largely accounted for by a distribution of hydroxyls in various environments, as shown by the ΔKS calculations with the $Si_{21}H_{20}$ cluster ($D$, $A$, and $F$ species binding energies span over 0.5 eV, see Table II). On the basis of the present ΔKS IP calculations we attribute the minority peak to bridging oxygens. As a matter of fact, calculations predict a chemical shift of 0.8 eV (to higher binding energy) between the dimer-inserted oxygen and the hydroxyl, when a $Si_9H_{12}$ cluster is used. When a $Si_{21}H_{20}$ cluster is used, the "bridging oxygen-hydroxyl" energy separation has a lower bound of 0.5 eV, the IP difference between H-Si-O-Si-H and the donor ($D$) hydroxyl, and an upper bound of 1.0 eV, the IP difference between H-Si-O-Si-H and the "free" ($F$) hydroxyl.

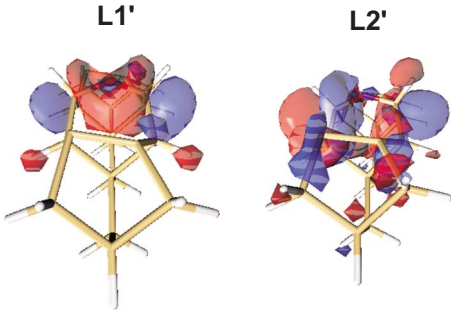


FIG. 12. (Color online) Core-excited inserted oxygen (H-Si-O-Si-H) calculated with a $Si_{21}H_{20}$ cluster. Contour plots of KS molecular orbitals ($L1'$,$L2'$) to which the electron is promoted. Note that $L1'$ is the LUMO.

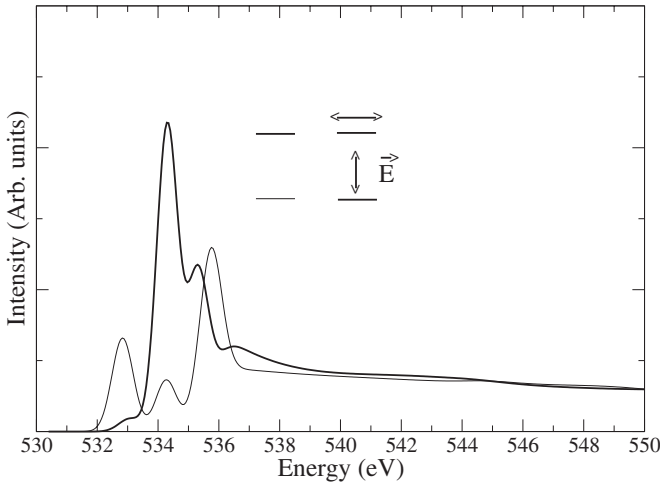


FIG. 13. Simulation of the O 1$s$ NEXAFS spectra for the inserted oxygen species (H-Si-O-Si-H) using the optimized geometry of the "$Si_{21}H_{20}$ plus (2H, O)" cluster. The $(1s)^1(L1')^{1/}(L2')^{1/2}$ FCH-UMOs potential is used. The fourfold symmetry of a two-domain silicon surface is taken into account. The thick (thin) line corresponds to **E** parallel (perpendicular) to the silicon surface.

Let us now turn our attention to the experimental O 1$s$ NEXAFS spectra, reported in Fig. 4. On the basis of the ΔKS calculations, the main absorption line at $h\nu$=534.6 is attributed to a manifold (hence its breadth) of transitions—essentially to orbitals of the $L2/L3$ type, deriving from the $2b_1^*$ molecular orbital of $H_2O$. The experimentally observed dichroism (the absorption is maximum when **E** is normal to the surface) can be explained if the OH axis azimuth tends to be oriented roughly normal to the Si-Si dimer axis azimuth. As shown by the simulated absorption curves, this can be an *average* orientation (in the case of unpaired OH), or this can be forced by hydrogen bonding between two adjacent OH lying on the same side of a dimer row (note also that O 1$s$ NEXAFS transition energies are marginally affected by a weak hydrogen bonding). On the other hand, the simulation [curve (c) of Fig. 6 and curve (c) of 10] shows that the first transition at 533 eV (associated to a $L1$ type orbital deriving from the $4a_1^*$ molecular orbital of water) should exhibit an absorption dichroism opposite to that of the 534 eV transitions—absorption stronger for **E** parallel to the surface. This dichroic behavior is not observed in the experimental curves, as the lower $h\nu$ line apparently does not show any polarization dependence. One must keep in mind the pres-

ence of minority species. For the H-Si-O-Si-H unit the first transition (of $4a_1^*$ type) at around 533 eV is more intense for **E** perpendicular to the surface. This compensates the depression of the first transition of the hydroxyl, arising at about the same energy.

We have already mentioned that the NEXAFS measured at a surface temperature of 300 K are not different from those recorded at a surface temperature of 150 K. This means that, on the average, the OH bond orientation is not strongly affected by a decrease in temperature.

## V. CONCLUSION

The system constituted by the Si(001)-$2\times1$ surface exposed to water molecules at room temperature has been chosen to single out the electron structure of the surface hydroxyls (SiOH). We have confronted here core-electron spectroscopy DFT calculations to synchrotron radiation O 1*s* XPS and (polarization-dependent) NEXAFS data. Using silicon clusters to mimic the silicon surface, various SiOH environments (unpaired and paired hydroxyls) have been examined. The impact of hydrogen bond on the calculated core-ionized and/or neutral core-excited states is examined, and compared to the limit case of the water dimer. The theoretical approach enables to label the main experimental NEXAFS transitions and to interpret their polarization-dependent dichroism.

As water dissociation on the surface can go beyond the formation of hydroxyls, the DFT electron structure of bridging oxygens (SiOSi) is calculated. It is predicted that the XPS line associated to the latter species is shifted by 0.5–1.0 eV to lower binding energy with respect to that of the hydroxyls. Then, on this basis, the reconstruction of the experimental O 1*s* XPS spectrum can provide the relative distribution of hydroxyls and of bridging oxygens (a minority species accounting for ca. 12% of the XPS spectral weight).

We believe that the present theoretical approach lays solid foundation for experimental core-electron spectroscopy studies of surface hydroxyls on silicon, which appear to play an important role in many technologically relevant processes. For instance, the study of the annealing of the water-reacted surface—leading to the formation of bridging oxygens or epoxy moieties—should strongly benefit from polarization dependent NEXAFS measurements. The $(H_2O)_2$ example also suggests that hydrogen bonding between SiOH and molecules such as molecular water, alcohols, amines, etc. should induce strong modifications in the XPS and NEXAFS spectra of the respective entities. Experimental and theoretical work is underway to examine these issues.

## ACKNOWLEDGMENTS

The authors are much indebted to Alfredo Pasquarello for enlightening discussions on silicon surface reactivity and for communicating us recent (yet unpublished) DFT periodic calculations on the $Si(001)/H_2O$ system.

*roch@ccr.jussieu.fr
†rangan@physics.rutgers.edu

[1] In the ALD process, metal precursors ($ML_n$) generally contain one metal atom *M* bound to *n* ligands *L*. When $H_2O$ is used as the oxygen source ligand-exchange involves breaking the metal-ligand bonds of the precursor and an O-H bond, and forming an *M*-O bond and a *L*-H bond. The first reaction step therefore consists in a reaction between surface hydroxyls and the metal precursor. See, for instance, Y. Widjaja and C. B. Musgrave, Appl. Phys. Lett. **81**, 304 (2002).

[2] A COSi linkage can be induced by a dehydrating reaction between OH on the Si(001) and OH in a carboxyl group (around half a monolayer of OH are produced by exposing the clean surface to $H_2O$), see K. Ihm, T.-H. Kanga, J. H. Han, S. Moon, C. C. Hwang, K.-J. Kima, H.-N. Hwang, C.-H. Jeon, H.-D. Kima, B. Kima, and C.-Y. Park, J. Electron Spectrosc. Relat. Phenom. **144-147**, 397 (2005).

[3] F. Rochet, F. Bournel, S. Carniato, G. Dufour, J.-J. Gallet, V. Ilakovac, K. L. Guen, S. Rangan, F. Sirotti, and S. Kubsky, Int. J. Nanosci. **6**, 85 (2007).

[4] According to Lee *et al.*, [S. S. Lee, J. Y. Baik, K. S. An, Y. D. Suh, J. H. Oh, and Y. Kim, J. Phys. Chem. B **108**, 15128 (2004)], an exposure of the clean surface to chlorine followed by an exposure to water at 230 °C leads to the formation of HO-Si-Si-OH units (2 OH decorating a silicon dimer). Using Si 2*p* x-ray photoemission spectroscopy with synchrotron radiation, these authors claim that *a monolayer of OH* forms on top of Si(001)-$2\times1$, with a limited O insertion between Si-Si bonds (the first oxidation state $Si^{1+}$ due to Si-OH bond formation is the *main* oxidation feature). On the other hand, S. Rivillon, R. T. Brewer, and Y. J. Chabal, Appl. Phys. Lett. **87**, 173118 (2005) using infrared spectroscopy did not find evidences for a replacement of the chlorine atoms by hydroxyls. Instead, silicon oxide is formed upon removal of the Si-Cl bond at ~325 °C.

[5] M. Henderson, Surf. Sci. Rep. **46**, 1 (2002).

[6] Y. J. Chabal and S. B. Christman, Phys. Rev. B **29**, 6974 (1984).

[7] In the very initial state of oxidation, the so-called C defects seen in STM images, would result from the bonding of the two (H,OH) fragments on adjacent dangling bonds of two Si dimers pertaining to the same row. See M. Z. Hossain, Y. Yamashita, K. Mukai, and J. Yoshinobu, Phys. Rev. B **67**, 153307 (2003).

[8] L. Andersohn and U. Köhler, Surf. Sci. **284**, 77 (1993).

[9] M. Chander, Y. Z. Li, J. C. Patrin, and J. H. Weaver, Phys. Rev. B **48**, 2493 (1993).

[10] C. Poncey, F. Rochet, G. Dufour, H. Roulet, F. Sirotti, and G. Panaccione, Surf. Sci. **338**, 143 (1995).

[11] A. B. Gurevich, B. B. Stefanov, M. K. Weldon, Y. J. Chabal, and K. Raghavachari, Phys. Rev. B **58**, R13434 (1998).

[12] The measurements were carried out at a surface temperature of 220 K to increase the signal to noise ratio. Y. Chabal (private communication).

[13] C. Larsson, A. Johnson, A. Flodström, and T. Madey, J. Vac. Sci. Technol. A **5**, 842 (1987).
[14] A. Johnson, M. M. Walczak, and T. E. Madey, Langmuir **4**, 282 (1988).
[15] 1 kcal/mol is equivalent to 43.36 meV.
[16] R. Konečný and D. Doren, J. Chem. Phys. **106**, 2426 (1997).
[17] F. N. Keutsch and R. J. Saykally, Proc. Natl. Acad. Sci. U.S.A. **98**, 10533 (2001).
[18] J. A. Odutola and T. R. Dyke, J. Chem. Phys. **72**, 5062 (1980).
[19] Y. Jung, C. H. Choi, and M. S. Gordon, J. Phys. Chem. B **105**, 4039 (2001).
[20] S. Bengió *et al.*, Phys. Rev. B **66**, 195322 (2002).
[21] M. Niwano, M. Terashi, M. Shinohara, D. Shoji, and N. Miyamoto, Surf. Sci. **401**, 364 (1998).
[22] K. Queeney, M. K. Weldon, Y. Chabal, and K. Raghavachari, J. Chem. Phys. **119**, 2307 (2003).
[23] G. R. Rao, Z.-H. Wang, H. Watanabe, M. Aoyagi, and T. Urisu, Surf. Sci. **570**, 178 (2004).
[24] S. Tanaka, K. Mase, S. Nagaoka, M. Nagasono, and M. Kamada, J. Chem. Phys. **117**, 4479 (2002).
[25] M. Cardona and L. Ley, *Photoemission in Solids* (Springer, Berlin, 1978).
[26] J. Stöhr, *NEXAFS Spectroscopy* (Springer, Berlin, 1992).
[27] At *K* edges, the orientation of the unoccupied *p*-like orbitals can be determined as the dipole absorption from a 1*s* level has a characteristic $\cos^2\delta$ dependence, where $\delta$ is the angle between the *p* orbital axis and the electric field **E** of the radiation. See Ref. 26 of this paper.
[28] Prior to the present paper, Tanaka and co-workers (Ref. 24) published an electron-ion coincidence spectroscopy study of the water dosed Si(001)-2×1 surface, in which an Auger yield O 1*s* NEXAFS spectrum of the surface is given. However, the photon bandwidth was much larger than in present case (~1.3 eV instead of ~0.25 eV). Moreover the dependence of the absorption intensity with the light incidence was not examined, as is the case in this work.
[29] S. Rangan, J.-J. Gallet, F. Bournel, S. Kubsky, K. Le Guen, G. Dufour, F. Rochet, F. Sirotti, S. Carniato, and V. Ilakovac, Phys. Rev. B **71**, 165318 (2005).
[30] S. Rangan, F. Bournel, J.-J. Gallet, S. Kubsky, K. Le Guen, G. Dufour, F. Rochet, F. Sirotti, S. Carniato, and V. Ilakovac, Phys. Rev. B **71**, 165319 (2005).
[31] F. Bournel, S. Carniato, G. Dufour, J.-J. Gallet, V. Ilakovac, S. Rangan, F. Rochet, and F. Sirotti, Phys. Rev. B **73**, 125345 (2006).
[32] M. Cavalleri, H. Ogasawara, L. G. M. Pettersson, and A. Nilsson, Chem. Phys. Lett. **364**, 363 (2002).
[33] V. C., I. Minkov, F. G. F. F. Guimaraes, A. Cesar, and H. Ågren, Chem. Phys. **312**, 311 (2005).
[34] L. Floreano *et al.*, Rev. Sci. Instrum. **70**, 3855 (1999).
[35] R. Gotter, A. Ruocco, A. Morgante, D. Cvetko, L. Floreano, F. Tommasini, and G. Stefani, Nucl. Instrum. Methods Phys. Res. A **467-468**, 1468 (2001).
[36] R. Nyholm and N. Mårtensson, Chem. Phys. Lett. **74**, 337 (1980).
[37] F. Rochet, C. Poncey, G. Dufour, H. Roulet, W. Rodrigues, M. Sauvage, J. C. Bouliard, F. Sirotti, and G. Panaccione, Surf. Sci. **326**, 229 (1995).
[38] E. Landemark, C. J. Karlsson, Y.-C. Chao, and R. I. G. Uhrberg, Phys. Rev. Lett. **69**, 1588 (1992).
[39] E. Pehlke and M. Scheffler, Phys. Rev. Lett. **71**, 2338 (1993).
[40] F. Jolly, F. Rochet, G. Dufour, C. Grupp, and A. Taleb-Ibrahimi, J. Non-Cryst. Solids **280**, 150 (2001).
[41] A. Pasquarello, M. S. Hybertsen, and R. Car, J. Vac. Sci. Technol. B **14**, 2809 (1996).
[42] A. Pasquarello, M. S. Hybertsen, and R. Car, Phys. Rev. Lett. **74**, 1024 (1995).
[43] E. Schröder-Bergen and W. Ranke, Surf. Sci. **236**, 103 (1990).
[44] D. J. Chadi, Phys. Rev. Lett. **43**, 43 (1979).
[45] L. C. Pauling, *The Nature of the Chemical Bond* (Cornell University Press, Ithaca, 1960).
[46] http://www.msg.ameslab.gov/GAMESS/GAMESS.html
[47] A. Becke, J. Chem. Phys. **98**, 5648 (1993).
[48] C. Lee, W. Yang, and R. G. Parr, Phys. Rev. B **37**, 785 (1988).
[49] D. R. Hamann, Phys. Rev. B **55**, R10 157 (1997).
[50] K. T. Queeney, Y. J. Chabal, and K. Raghavachari, Phys. Rev. Lett. **86**, 1046 (2001).
[51] J.-H. Guo, Y. Luo, A. Augustsson, S. Kashtanov, J.-E. Rubensson, D. K. Shuh, H.Ågren, and J. Nordgren, Phys. Rev. Lett. **91**, 157401 (2003).
[52] M. Koné, B. Illien, J. Graton, and C. Laurence, J. Phys. Chem. A **109**, 11907 (2005).
[53] W. Klopper, J. G. C. M. van Duijneveldt-van de Rijdt, and F. B. van Duijneveldt, Phys. Chem. Chem. Phys. **2**, 2227 (2000).
[54] S. Carniato, V. Ilakovac, J. J. Gallet, E. Kukk, and Y. Luo, Phys. Rev. A **71**, 022511 (2005).
[55] L. Triguero, J. Electron Spectrosc. Relat. Phenom. **104**, 195 (1999).
[56] T. Ziegler, A. Rauk, and E. J. Baerends, Theor. Chim. Acta **43**, 261 (1977).
[57] Note that the influence of the silicon cluster size on the NEXAFS and IP calculated transitions has been examined in the case of the acetonitrile/Si(001) (Ref. 30 of this paper) and benzonitrile/Si(001) (Ref. 29 of this paper) of this systems. Increasing the cluster size has no effect on the NEXAFS transitions calculated with the ΔKS method. On the other hand, the IP energy typically diminishes by 0.2-0.3 eV when the cluster size is multiplied by a factor of about 2 (from a $Si_9H_{12}$ single-dimer cluster to a $Si_{21}H_{20}$ three-dimer cluster).
[58] P. W. Langhoff, Chem. Phys. Lett. **22**, 60 (1973).
[59] R. Sankari, M. Ehara, H. Nakatsuji, Y. Senba, K. Hosawaka, H. Yoshida, A. D. Fanis, Y. Tamenori, S. Aksela, and K. Ueda, Chem. Phys. Lett. **380**, 647 (2003).
[60] R. D. Smardon and G. Srivastava, Surf. Sci. **584**, 161 (2005).
[61] J.-H. Cho, K. S. Kim, S.-H. Lee, and M.-H. Kang, Phys. Rev. B **61**, 4503 (2000).
[62] *RT* (*kT*) is equal to 0.298 kcal/mol (12.9 meV) at 150 K and 0.596 kcal/mol (25.8 meV) at 300 K, comparable to the trans-to-gauche energy barrier of 0.5–0.6 kcal/mol (21.7–26.0 meV).
[63] F. Giustino and A. Pasquarello (private communication).
[64] The H bond lengths we calculate with the DFT/B3LYP approach—whatever the size of basis set—remain much longer than those calculated with the MP2 method using the HW(*d*) basis set and the $Si_{48}H_{36}$ cluster. This may be a problem of basis set size in the latter case, as for a smaller two-dimer cluster a MP2 calculation with a DZV(*d*) basis set leads to a $d_{H(D)O(A)}$ value of 2.32 Å (Ref. 19 of this paper).
[65] The IP decreases by about 0.25 eV passing from a bridging Si-O-Si species in a single-dimer cluster to a bridging oxygen

placed at the central dimer of the three-dimer cluster (see Table V). Therefore the IP of an isolated OH placed at the center of a three-dimer cluster should be that calculated for a single-dimer cluster (537.79 eV) diminished by 0.25, that is 537.65 eV.

[66] M. K. Weldon, B. B. Stefanov, K. Raghavachari, and Y. J. Chabal, Phys. Rev. Lett. **79**, 2851 (1997).

[67] B. R. Trenhaile, A. Agrawal, and J. H. Weaver, Appl. Phys. Lett. **89**, 151917 (2006).

[68] B. B. Stefanov and K. Raghavachari, Surf. Sci. **389**, L1159 (1997).

[69] H. Watanabe, S. Nanbu, Z. H. Wang, and M. Aoyagi, Chem. Phys. Lett. **424**, 133 (2006).